

**Figure S1. (Related to Figure 1)**

(A) Targeting diagram, including locations of exons/introns, loxP (triangle) and FRT (rectangle) sites, PCR primers (Dlx5fgt.52, Dlx5fgt.53, Dlx5fgt.31), Southern blot enzymes, and Southern blot probes (grey boxes: \*, \*\*, \*\*\*) and restriction enzyme sites (B: BamHI; S: SacI).

(B) Southern blot on DNA from *Dlx5<sup>fllox/+</sup>* and wild-type mice: BamHI digest hybridized with the Dlx5-Spe/Bam (\*\*) probe labels a wild type band of 6251 bp and a *Dlx5<sup>fllox</sup>* band of 2260 bp.

(C) PCR genotyping from a *Dlx5<sup>fllox/+</sup>* intercross showing PCR fragments of 328 bp (wild type) and 520 bp (*Dlx5<sup>fllox</sup>*). PCR from heterozygous animals generated a doublet as shown.

(D) PCR genotyping of *Dlx5<sup>Δ</sup>* and control mice: Dlx5fgt.53 and Dlx5fgt.31 amplify a 470bp fragment from the allele following Cre-mediated deletion of the floxed region. Data not shown: Southern with genomic DNA from *Dlx5<sup>fllox/+</sup>* (neo<sup>+</sup>) mice. SacI digest with Dlx5dn2 probe (+ 4.4kb, f 3.4kb, Δ 10.2 kb), XmnI digest with exon 3 probe (+ 9.2 kb, f 11.3 kb).

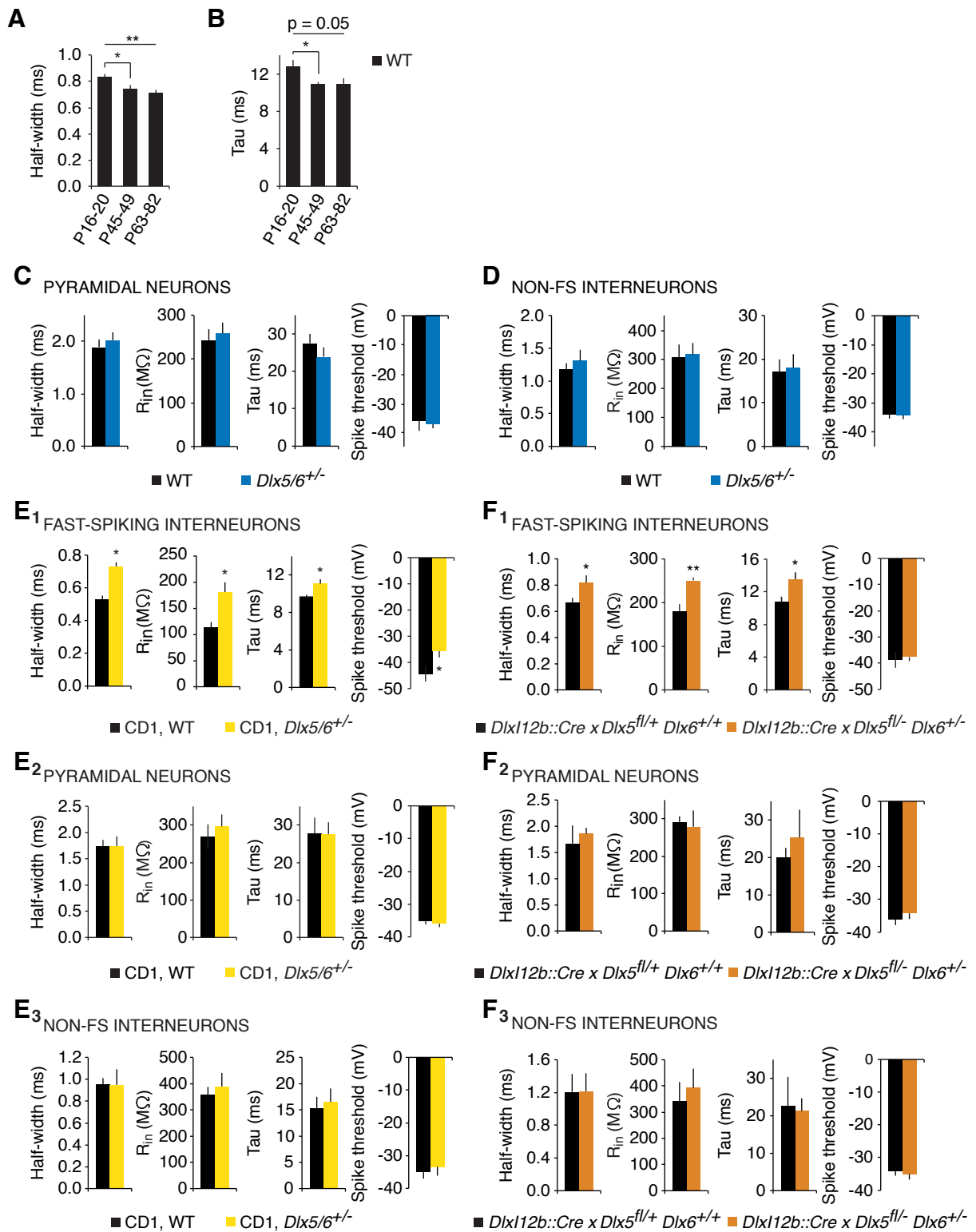


**Figure S2. (Related to Figure 1)**

(A) The action potential half-width of WT FSINs decreases as the animal matures from P16-20 (juvenile, n = 8) to P45-49 (adolescent, n = 9) to P63-82 (adult, n = 23) in response to brief current pulses.

(B) The membrane time constant of WT FSINs decreases as the animal matures from P16-20 (juvenile, n = 8) to P45-49 (adolescent, n = 9) to P63-82 (adult, n = 23) in response to brief current pulses.

(C) The action potential half-width, input resistance, membrane time constant, and action potential threshold for pyramidal neurons in adult (P63-82) wild-type and *Dlx5/6*<sup>+/-</sup> mice, based on the responses to a series of current injections (n = 6 neurons per genotype).

(D) The action potential half-width, input resistance, membrane time constant, and action potential threshold for non-fast-spiking interneurons in P63-82 wild-type and *Dlx5/6*<sup>+/-</sup> mice, based on the responses to a series of current injections (n = 11-13 interneurons per genotype).

(E) The action potential half-width, input resistance, membrane time constant, and action potential threshold in adult (>8.5 week old) WT and *Dlx5/6*<sup>+/-</sup> mice that have been backcrossed to CD1 for at least 6 generations, based on responses to a series of current injections in FSINs (E<sub>1</sub>), pyramidal neurons (E<sub>2</sub>), and non-FS interneurons (E<sub>3</sub>). The intrinsic properties of FSINs are abnormal in *Dlx5/6*<sup>+/-</sup> mice on a CD1 background (WT: n = 8; *Dlx5/6*<sup>+/-</sup>: n = 6), whereas intrinsic properties were similar for pyramidal neurons (WT: n = 7; *Dlx5/6*<sup>+/-</sup>: n = 15) and non-FS interneurons (WT: n = 9; *Dlx5/6*<sup>+/-</sup>: n = 8).

(F) The action potential half-width, input resistance, membrane time constant, and action potential threshold for non-fast-spiking interneurons in adult (>9.1 week old) mutant mice (*Dlx12b::Cre x Dlx5*<sup>fl/+</sup> *Dlx6*<sup>+/+</sup>) and controls (*Dlx12b::Cre x Dlx5*<sup>fl/-</sup> *Dlx6*<sup>+/+</sup>). Intrinsic properties were calculated based on the responses to a series of current injections in FSINs (F<sub>1</sub>), pyramidal neurons (F<sub>2</sub>), and non-FS interneurons (F<sub>3</sub>). The intrinsic properties of FSINs are abnormal in *Dlx12b::Cre x Dlx5*<sup>fl/-</sup> *Dlx6*<sup>+/-</sup> mice (n = 6 cells from 3 mice) compared to controls (n = 6), but intrinsic properties were similar in pyramidal neurons (mutants: n = 4; controls: n = 8) and non-FS interneurons (mutants: n = 7; controls: n = 4).

All data show means ± SEM and are analyzed using two-tailed Student's unpaired t-tests. \*p < 0.05, \*\*p < 0.01.

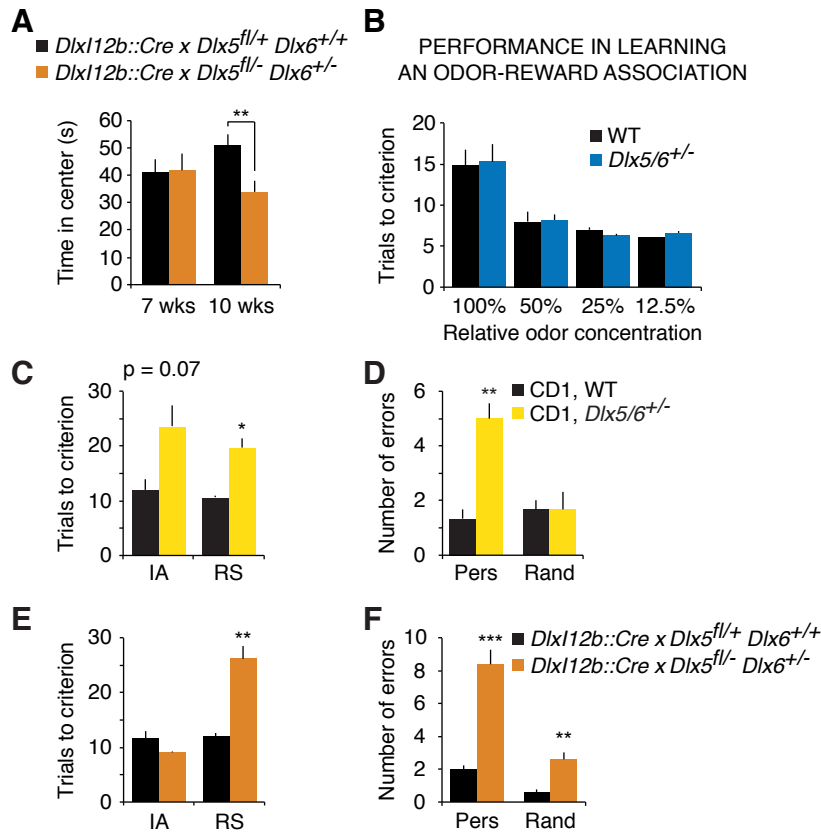


**Figure S3. (Related to Figure 2)**

(A) *Dlx12b::Cre x Dlx5<sup>fl/-</sup> Dlx6<sup>+/-</sup>* mice exhibit a post-adolescent increase in anxiety. In the open field test, 7 week old *Dlx12b::Cre x Dlx5<sup>fl/+</sup> Dlx6<sup>+/+</sup>* mice and age-matched controls (*Dlx12b::Cre x Dlx5<sup>fl/+</sup> Dlx6<sup>+/+</sup>* mice) ( $n = 5$  mice per genotype) spend similar amounts of time in the center of the field, but after 10 weeks of age, *Dlx12b::Cre x Dlx5<sup>fl/-</sup> Dlx6<sup>+/-</sup>* mice spend less time in the center than controls mice ( $n = 5$  controls and 6 *Dlx12b::Cre x Dlx5<sup>fl/-</sup> Dlx6<sup>+/-</sup>* mice). All data show means  $\pm$  SEM and analyzed using two-tailed, unpaired Student's *t*-tests. \*\* $p < 0.01$ .

(B) After training adult *Dlx5/6<sup>+/-</sup>* mice or their wild-type littermates to associate a coriander odor with a food reward, we tested mice by continuing to present two bowls, only one of which contained the food reward and coriander odor. We progressively decreased the concentration of the coriander odor (100% to 50% to 25% to 12.5%, relative to the dose used in the rule-shifting task). Adult *Dlx5/6<sup>+/-</sup>* were not impaired, relative to wild-type mice, in their ability to detect the coriander odor and find the food reward. All data show means  $\pm$  SEM from 5 WT and 7 *Dlx5/6<sup>+/-</sup>* mice.

(C-F) Adult *Dlx5/6<sup>+/-</sup>* mice backcrossed to CD1 for at least 6 generations and *Dlx12b::Cre x Dlx5<sup>fl/-</sup> Dlx6<sup>+/-</sup>* mice exhibit impaired rule shifting.

(C) Performance of adult (>10 week old) CD1, *Dlx5/6<sup>+/-</sup>* mice ("CD1, *Dlx5/6<sup>+/-</sup>*", yellow) and their wild-type littermates ("CD1, WT", black, left columns) on the rule-shifting portion of the task ( $n = 3$  mice per genotype, both genders). During the rule-shifting portion of the task, CD1, *Dlx5/6<sup>+/-</sup>* mice required significantly more trials to reach the learning criterion than their wild-type littermates.

(D) During the rule-shifting portion of the task, adult CD1, *Dlx5/6<sup>+/-</sup>* mice made a preponderance of perseverative errors, and made more perseverative errors than their wild-type littermates ( $n = 3$  mice per genotype).

(E) During the rule-shifting portion of the task, adult (>11 week old) *Dlx12b::Cre x Dlx5<sup>fl/-</sup> Dlx6<sup>+/-</sup>* mice required significantly more trials to reach the learning criterion than did control mice (*Dlx12b::Cre x Dlx5<sup>fl/+</sup> Dlx6<sup>+/+</sup>*) ( $n = 5$  mice per genotype).

(F) Adult *Dlx12b::Cre x Dlx5<sup>fl/-</sup> Dlx6<sup>+/-</sup>* mice made a preponderance of perseverative errors, and made more perseverative errors than did control mice ( $n = 5$  mice per genotype) during the rule-shifting portion of the task.

All data show means  $\pm$  SEM and are analyzed using two-tailed Student's *t*-tests. \* $p < 0.05$ , \*\* $p < 0.01$ , \*\*\* $p < 0.001$ .

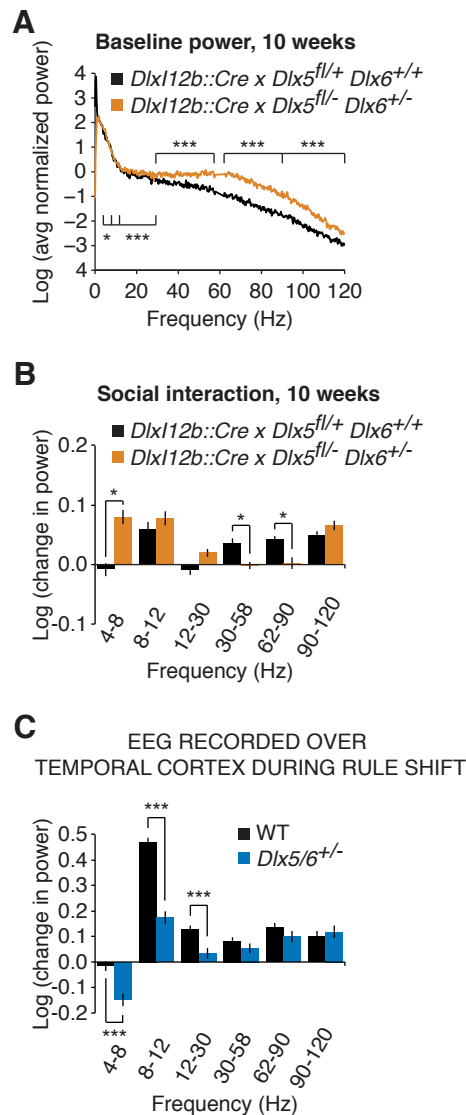


**Figure S4. (Related to Figure 4)**

(A) *Dlx112b::Cre x Dlx5<sup>fl/-</sup> Dlx6<sup>+/-</sup>* mice exhibit abnormal baseline  $\gamma$  oscillations and deficient task-evoked prefrontal  $\gamma$  oscillations during social interaction. Log transform of the averaged, normalized power spectrum for prefrontal EEG recordings from adult (>10 week old) *Dlx112b::Cre x Dlx5<sup>fl/-</sup> Dlx6<sup>+/-</sup>* (orange trace) and wild-type (*Dlx112b::Cre x Dlx5<sup>fl/+</sup> Dlx6<sup>+/+</sup>*) (black trace) mice. For this plot, the power spectrum from each mouse was normalized by the sum of all values from 0-120 Hz (excluding 58-62 Hz). Note the increased power in the  $\gamma$  range.

(B) During periods of social interaction, adult wild-type mice show an increase in the power of prefrontal  $\gamma$  oscillations (30-90 Hz, relative to baseline) compared to no change or a slight decrease in prefrontal  $\gamma$  power in age-matched control (*Dlx112b::Cre x Dlx5<sup>fl/+</sup> Dlx6<sup>+/+</sup>*) mice. All data show means  $\pm$  SEM from 4 control and 5 *Dlx112b::Cre x Dlx5<sup>fl/-</sup> Dlx6<sup>+/-</sup>* mice. \* $p < 0.05$ , \*\*\* $p < 0.001$ .

(C) Abnormal rule shifting-evoked gamma oscillations in *Dlx5/6<sup>+/-</sup>* mice are region specific. Task-evoked gamma oscillations recorded over temporal cortex during rule shifting are not appreciably different between adult wild-type and *Dlx5/6<sup>+/-</sup>* mice ( $n = 8$  mice per genotype). Asterisks above pairs of black and blue bars indicate cases in which power in a frequency band was significantly different between WT and *Dlx5/6<sup>+/-</sup>* mice.

All data show means  $\pm$  SEM and are analyzed using two-tailed Student's unpaired t-tests or 2-way ANOVA or repeated measures ANOVA. \*\*\* $p < 0.001$ .

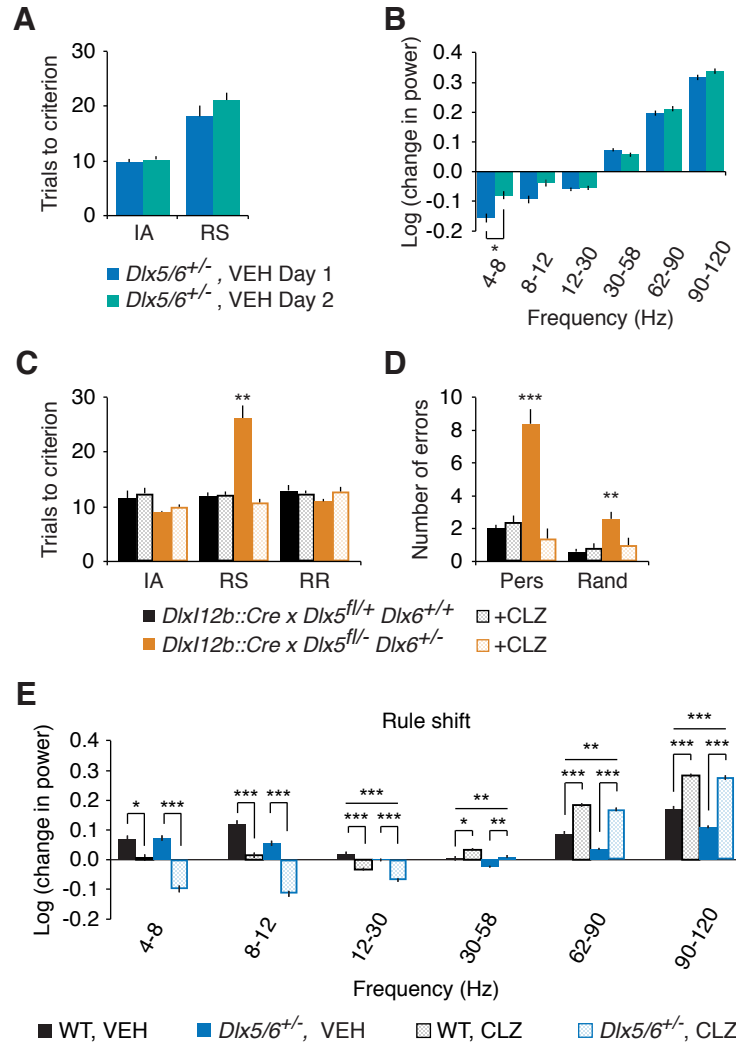


**Figure S5. (Related to Figure 6)**

(A) Task-evoked gamma oscillations in *Dlx5/6*<sup>+/-</sup> mice are similar over two consecutive days of the rule shifting task. There is no change in rule-shifting evoked  $\gamma$  oscillations over the two days of vehicle treatment in a cohort of adult, *Dlx5/6*<sup>+/-</sup> mice (train versus task,  $n = 5$  mice per genotype). All data shown are means  $\pm$  SEM. \* $p < 0.05$ .

(B) Low-dose clonazepam (CLZ) rescues deficits in rule shifting in adult *Dlx12b::Cre x Dlx5*<sup>fl/-</sup> *Dlx6*<sup>+/-</sup> mice. CLZ completely normalized the number of trials required for adult *Dlx12b::Cre x Dlx5*<sup>fl/-</sup> *Dlx6*<sup>+/-</sup> mice to learn the rule-shifting task ( $n = 5$  mice per genotype). The number of trials to learn the initial association and the rule reversal task were not affected.

(C) CLZ led to a complete normalization of the number of perseverative and random errors made by the adult *Dlx12b::Cre x Dlx5*<sup>fl/-</sup> *Dlx6*<sup>+/-</sup> mice during rule shifting ( $n = 5$  mice per genotype). \*\* $p < 0.01$ , \*\*\* $p < 0.001$ .

(D) CLZ rescues task-evoked oscillations in the upper  $\gamma$  range (62-90 Hz) during rule-shifting in *Dlx5/6*<sup>+/-</sup> mice. Task-evoked oscillations (62-90 Hz) in *Dlx5/6*<sup>+/-</sup> mice were significantly larger in CLZ than in vehicle, and after CLZ treatment, the task-evoked increase in 62-90 Hz power was similar for *Dlx5/6*<sup>+/-</sup> and WT mice.

(E) Data from Figures 6D and 6E have been combined into a single plot, comparing rule shift-evoked oscillations in various frequency bands for WT or *Dlx5/6*<sup>+/-</sup> mice treated with vehicle (VEH) or CLZ. Asterisks indicate significant differences either between VEH- and CLZ-treated mice of the same genotype, or between VEH-treated WT and mutant mice.

All data show means  $\pm$  SEM and are analyzed using two-tailed Student's t-tests or repeated measures ANOVA.

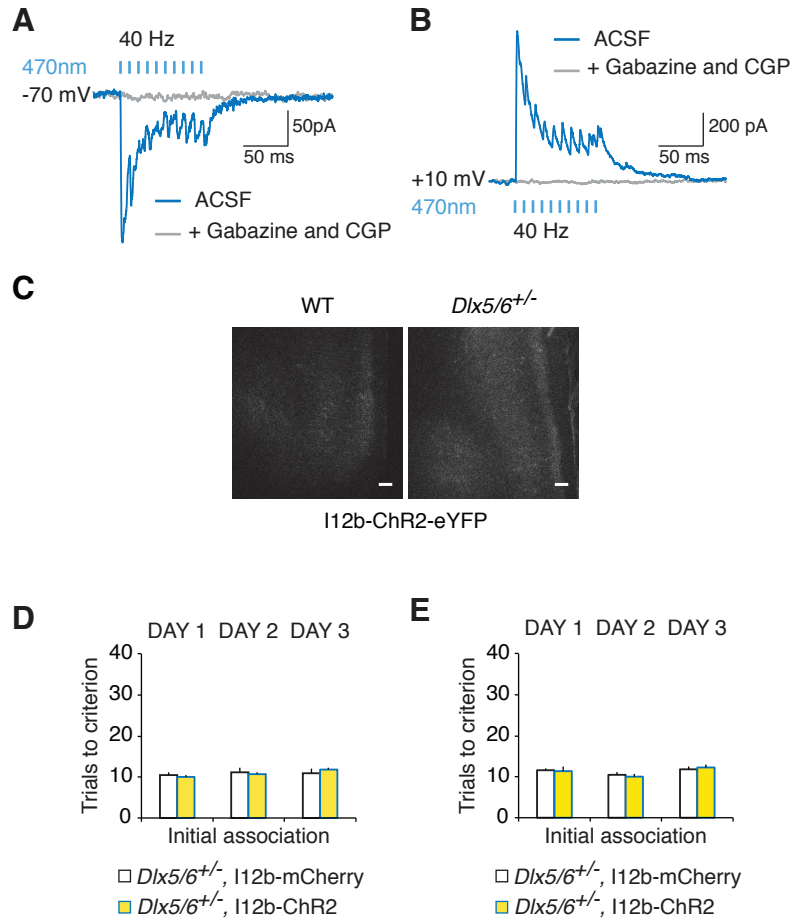


**Figure S6. (Related to Figure 7)**

(A-B) I12b-driven ChR2 expression occurs specifically within GABAergic neurons. Synaptic currents recorded from prefrontal pyramidal neurons during 40 Hz optogenetic stimulation in slices from mice injected with AAV carrying I12b-ChR2-eYFP, which drives ChR2 expression under control of the I12b enhancer. All optogenetically evoked synaptic currents (blue) were blocked after application of the GABAergic antagonists gabazine and CGP35348 (black).

(C) Images of I12b-ChR2-eYFP expression in both WT and *Dlx5/6<sup>+/-</sup>* mice (scale bar = 100  $\mu$ m).

(D) Performance of adult *Dlx5/6<sup>+/-</sup>* mice on the initial association portion of the task, for Days 1-3 of the pre-stim, 40 Hz opto-stim, and post-stim experiment, respectively, in animals injected with either I12b-ChR2 (n = 6-7) and I12b-mCherry (n = 4).

(E) Performance of adult *Dlx5/6<sup>+/-</sup>* mice on the initial association portion of the task, for Days 1-3 of the pre-stim, 12.5 Hz burst opto-stim, and 40 Hz opto-stim experiment, respectively, in animals injected with either I12b-ChR2 (n = 5) and I12b-mCherry (n = 4). Data show means  $\pm$  SEM and are analyzed using two-tailed Student's unpaired t-test.

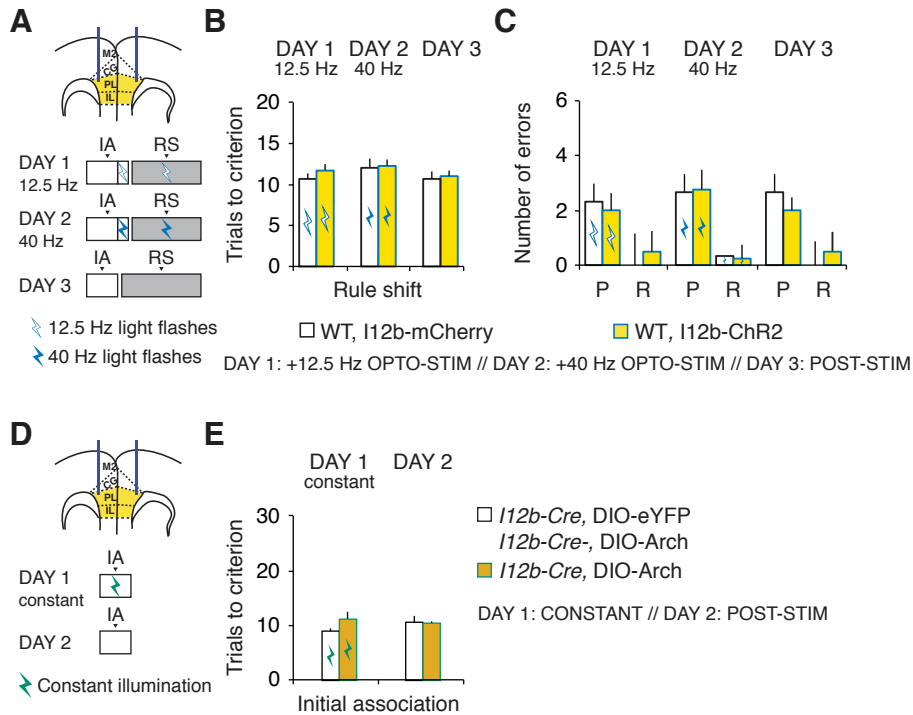


**Figure S7. (Related to Figure 7)**

(A) Schematic illustrating the design of experiments in which animals perform the IA and RS in the presence of 12.5 Hz optogenetic stimulation on Day 1, then receive 40 Hz optogenetic stimulation of PFC interneurons on Day 2, and no optogenetic stimulation on Day 3.

(B-C) The 12.5 Hz stimulation depicted in (A) fails to alter either the number of trials required to learn the rule shift, or the number of perseverative errors (C). 40 Hz stimulation also does not alter rule shifting in ChR2-expressing mice (n = 5) compared to mCherry-expressing controls (n = 4), or the number of perseverative errors (C). In the absence of optogenetic stimulation on Day 3, no changes are observed (B-C).

(D) Schematic illustrating the design of experiments in which animals perform the IA in the presence of constant illumination on Day 1, then no optogenetic stimulation on Day 2.

(E) Constant inhibition of PFC interneurons does not affect the initial association in Arch-expressing mice (n = 4) compared to *I12b-Cre*, DIO-eYFP or *I12b-Cre-*, DIO-Arch expressing controls (n = 3).

All data show means ± SEM and are analyzed using two-tailed Student's t-tests.

## SUPPLEMENTAL EXPERIMENTAL PROCEDURES

**Subjects.** *Dlx5/6*<sup>+/-</sup> mice were generated as previously described (Wang et al., 2010), and either maintained on a mixed CD1 and C57Bl/6 background, or backcrossed to CD1 for at least 6 generations. All experiments were done using *Dlx5/6*<sup>+/-</sup> mice and their age-matched wild-type littermates or *Dlx112b::Cre × Dlx5<sup>fl/-</sup>Dlx6<sup>+/-</sup>* conditional knockout mice and their age-matched control littermates (*Dlx112b::Cre × Dlx5<sup>fl/+</sup>Dlx6<sup>+/+</sup>*) or *Dlx112b-Cre (I12b-Cre)* mice and their age-matched littermate controls (*I12b-Cre* mice injected with control virus or *I12b-Cre*-negative mice). Unless otherwise noted, subjects were fed *ad libitum* and reared in normal lighting conditions (12/12 light/dark cycle). All experiments were conducted in accordance with procedures established by the Administrative Panels on Laboratory Animal Care at the University of California, San Francisco.

### **Generation of *Dlx112b::Cre × Dlx5<sup>fl/-</sup>Dlx6<sup>+/-</sup>* conditional knockout mice.**

Recombineering at the UCSF transgenic core was used to generate the *Dlx5<sup>lox</sup>* targeting construct, in which exons 2 and 3 were flanked by loxP sites, and an FRT-flanked neomycin-resistance cassette was introduced after exon 3. The long arm of homology (LA) extended 8813bp upstream of exon 1, and the short arm of homology (SA) extended approximately 1.7kb downstream of the second loxP site. The targeting vector was linearized and electroporated into embryonic stem (ES) cells. Following neomycin selection, correctly-targeted ES cell clones were identified by PCR using the following primers: *Dlx5-con-scr-s* (ATTTCGACCATGGAAACTGC), *Dlx5-c-scr-as*

(GACATGCGCTTGGTACACAC), Dlx5-c-scr-s (TGCTATACGAAGTTATTAGGTGGA); product sizes 2385 bp (wild-type) and 1869 bp (flox).

Correctly-targeted ES cells were injected into blastocysts to generate chimeric mice. After germline transmission, the targeted allele was verified in *Dlx5<sup>flox/+</sup>* mice by Southern blot analysis with an internal exon 3 probe (\*) and two probes external to the targeted region (\*\*, \*\*\*) (fig. S1). Southern blot probes were generated by PCR amplification from C57Bl/6 genomic DNA using the following primers: \* (Dlx5-intr2.51 [ggtagttagttatcagggcagg], Dlx5-ex3.31 [aaccagcacaactgtagtcc]), \*\* (Dlx5dnSpeI.51 [actagtagaggtctcttgaattgg], Dlx5dnBam.31 [acaggaatgcagcttcctcgg]), and \*\*\* (Dlx5-dn.52 [cacctacccgggagtcagtc], Dlx5-dn.32 [gaggcactggatccaagaggt]).

The neomycin resistance cassette for ES cell selection was excised *in vivo* by crossing *Dlx5<sup>flox/+</sup>* mice to hActB::Flpe deleter mice (Rodriguez et al., 2000). Deletion of the neomycin cassette was confirmed by PCR and Southern analysis (data not shown) and Flpe was subsequently bred out of the line. *Dlx5<sup>flox</sup>* (neo<sup>-</sup>) mice were subsequently genotyped using primers that flank the second loxP site (Dlx5fgt.52 [ctacatttctcctaccgtgtgt], Dlx5fgt.31 [cccagtacttcaggttcactat]).

To confirm the functionality of the allele, *Dlx5<sup>flox</sup>* mice were bred to beta actin mice::Cre mice, which ubiquitously express Cre (Lewandoski et al., 1997). PCR analysis demonstrated that the floxed region of the *Dlx5* allele was deleted in the resultant *Dlx5<sup>+/-</sup>*; beta actin::Cre mice, as expected (PCR primers Dlx5fgt.31, Dlx5gt.53 [gtgaaatcaagcagccctagtg], product size 470 bp. Skeletal preparations with Alizarin red and Alcian blue staining confirmed that *Dlx5<sup>+/-</sup>* embryos generated from these mice had

craniofacial abnormalities similar to those reported previously for *Dlx5*<sup>-/-</sup> animals (data not shown) (Depew et al., 1999).

**Slice preparation.** Slice preparation and intracellular recording followed our published protocol (Sohal and Huguenard, 2005). Coronal slices, 250  $\mu\text{m}$  thick, from P16-P20, P45-P49, and P63-P88 mice of either sex were cut in a chilled slicing solution in which  $\text{Na}^+$  was replaced by sucrose, then incubated in warmed ACSF at 30-31°C for 15 minutes and then at least one hour at room temperature before being used for recordings. ACSF contained (in mM): 126 NaCl, 26  $\text{NaHCO}_3$ , 2.5 KCl, 1.25  $\text{NaH}_2\text{PO}_4$ , 1  $\text{MgCl}_2$ , 2 CaCl, and 10 glucose. Slices were secured by placing a harp along the midline between the two hemispheres.

**Intracellular recording.** Somatic whole-cell patch recordings were obtained from visually identified neurons in layer 5 of infralimbic or prelimbic cortex using differential contrast video microscopy on an upright microscope (BX51WI; Olympus). Recordings were made using a Multiclamp 700A (Molecular Devices). Patch electrodes (tip resistance = 2–6 M $\Omega$ ) were filled with the following (in mM): 130 K-gluconate, 10 KCl, 10 HEPES, 10 EGTA, 2 MgCl, 2 MgATP, and 0.3 NaGTP (pH adjusted to 7.3 with KOH). All recordings were at 32.5 $\pm$ 1°C. Series resistance was usually 10–20 M $\Omega$ , and experiments were discontinued above 30 M $\Omega$ .

In experiments in which GABA<sub>A</sub> and GABA<sub>B</sub> receptors were blocked, drugs were bath applied at the following concentrations (in  $\mu\text{M}$ ): 10 gabazine (Sigma), 5 CGP35348 (Sigma). These pharmacology experiments were performed blind to genotype.

**Injection of virus for DlxI12b expression.** To visually identify interneuron subtypes, we injected an adeno-associated virus (AAV) vector that drives mCherry expression using the DlxI12b enhancer, which marks interneurons (Lee et al., 2014; Potter et al., 2009) (hereafter abbreviated as I12b). We injected 0.5  $\mu$ l of virus following previously-described procedures (Sohal et al., 2009). We waited at least 4 weeks after virus injection before preparing brain slices. Coordinates for injection into mPFC were (in millimeters relative to bregma): 1.7 anterior-posterior (AP), 0.3 mediolateral (ML), and -2.75 dorsoventral (DV).

**Injection of virus for ChR2 expression.** To express ChR2 specifically in interneurons, we used an adeno-associated virus (AAV) that drives I12b-dependent expression of a ChR2-eYFP fusion protein. To produce the interneuron-specific channelrhodopsin, MluI and BamHI compatible sticky ends were introduced to the DlxI12b-BG sequence with PCR. The AAV-CamKII-ChR2-eYFP (from Karl Deisseroth) was then cut with MluI/BamHI and ligated to the PCR insert to exchange the CamKII promoter for DlxI12b-BG. Virus was packaged by UNC Vector Core with serotype AAV5. For the *in vitro* slice experiments, we injected 0.75  $\mu$ l of virus following previously-described procedures (Sohal et al., 2009), then waited at least 4 weeks after virus injection before preparing brain slices. For experiments in which we recorded from ChR2-negative pyramidal neurons while stimulating ChR2 in interneurons (labeled using I12b), we injected virus into the medial PFC (mPFC) and verified that we observed fluorescent soma on the injected side (which was the location for recording). Coordinates for

injection into mPFC were (in millimeters relative to bregma): 1.7 anterior-posterior (AP), 0.3 mediolateral (ML), and -2.75 dorsoventral (DV). For the *in vivo* optogenetic stimulation experiments, we injected 1  $\mu$ l of I12b-dependent ChR2-eYFP or I12b-dependent mCherry virus in each hemisphere, then waited 5.5 weeks after virus injection before beginning behavioral experiments. These injections as well as the subsequent behavioral assays were performed blind to the identity of the particular virus (ChR2 vs. mCherry) that was used.

As a control for possible confounding differences in ChR2-eYFP expression, we confirmed that levels of eYFP fluorescence were not decreased – actually they were slightly higher – in *Dlx5/6*<sup>+/-</sup> mice compared to WT (Figure S6C).

**Injection of virus for Arch expression.** To express archaerhodopsin (Arch) specifically in interneurons, we used an adeno-associated virus (AAV) that is a DIO-eArch3.0-eYFP construct driven by the ubiquitous EF1 $\alpha$  promoter and injected it into *Dlx1/2b-Cre* mice (Potter et al., 2009). Virus was packaged by UNC Vector Core with serotype AAV5. Coordinates for injection into mPFC were (in millimeters relative to bregma): 1.7 anterior-posterior (AP), 0.3 mediolateral (ML), and -2.75 dorsoventral (DV). We injected 1.5  $\mu$ l of DIO-Arch3.0-eYFP or DIO-eYFP virus in each hemisphere, then waited 5.5 weeks after virus injection before beginning behavioral experiments. These injections as well as the subsequent behavioral assays were performed blind to the identity of the particular virus (Arch or eYFP) that was used.

***In vitro* ChR2 stimulation.** We stimulated ChR2 in interneurons using ~4-5mW flashes

of light generated by a Lambda DG-4 high-speed optical switch with a 300W Xenon lamp (Sutter Instruments), and an excitation filter set centered around 470 nm, delivered to the slice through a 40x objective (Olympus). Illumination was delivered across a full high-power (40x) field. To measure inhibitory currents, we made voltage-clamp recordings at a holding potential of +10 mV while stimulating ChR2 using trains of light flashes (10 flashes, 5 msec / flash, 40 Hz). Experiments were performed blind to genotype.

**Analysis of intrinsic properties.** Intrinsic properties were calculated based on the current clamp responses to a series of 250 msec current pulse injections from -200 to 450 pA (50 pA/increment). Input resistance was calculated from the voltage response to a -50 pA, 250 msec current pulse. Spiking properties were calculated based on the response to a current pulse that was 100 pA above the minimal level that elicited spiking. Spike half-width was defined as the width (in msec) at half-maximal amplitude. The adaptation ratio was the ratio between the first and last interspike interval. The spike threshold was defined as the point between two spikes at which  $d^3V/dt^3$  was maximal. The slope of the firing rate vs. input current ( $f-I$ ) relationship was calculated from the responses to current pulses that were above the threshold to elicit spiking, up to 450 pA.

As described above, we identified interneurons based on the expression of mCherry driven by AAV and the Dlx112b enhancer (Potter et al., 2009). This enhancer element marks a diverse population of interneuron subtypes. Recorded interneurons were therefore subdivided into fast-spiking (FS) or non-FS based on electrophysiological properties. Specifically, we classified an interneuron as fast-spiking if the adaptation ratio

was  $<1.3$ , and the input resistance was  $<350$  MOhms. To confirm that the well-established correspondence between PV expression and FS electrophysiological properties is maintained in *Dlx5/6*<sup>+/-</sup> mice and their WT counterparts, we filled a subset of recorded interneurons with biocytin ( $n = 5$  in each genotype) and stained for PV. Based on these electrophysiological criteria, almost all PV-expressing neurons (9/10) were classified as fast-spiking, and the intrinsic properties of these PV-expressing neurons were not significantly different from those of the larger population of fast-spiking interneurons that were identified based on electrophysiologic properties. Indeed, within each genotype, there were no significant differences in adaptation ratio, slope of the *f-I* relationship, input resistance, membrane time constant, spike half-width, or spike threshold between the immunohistochemically-identified PV-expressing cells ( $n = 5$  for each genotype) and electrophysiologically-identified FSINs ( $n = 16-23$  for each genotype;  $p = 0.23-0.94$ ).

All data were analyzed using Student's two-tailed, unpaired *t*-tests.

**Biocytin fills, PV staining, and confocal imaging.** For experiments in which we confirmed the molecular identity of recorded cells by subsequent staining for PV, the intracellular solution contained 0.3% biocytin. Cells filled with biocytin were fixed overnight in a buffered solution containing 4% paraformaldehyde. To stain for PV, slices were first washed four times in 0.1 M PBS, then washed three times in PBS with 0.3% Triton X-100. Next, slices were incubated for two days with mouse monoclonal anti-PV (1:5000) in blocking solution (normal goat serum, 0.3% Triton X-100, 2% BSA, PBS), washed six times in PBS with 0.3% Triton X-100, and then incubated with AlexaFluor

488 goat anti-mouse (1:200) in blocking solution for 3 h. To visualize filled cells, CF405M Streptavidin (1:2000) was also added for the 3 h incubation. Finally, slices were washed 6 times in PBS with 0.3% Triton X-100, then 4 times in PBS before mounting. All imaging was performed on a Zeiss LSM510.

**Open-field test.** An individual mouse was placed near the wall-side of 50 x 50 cm open-field arena, and the movement of the mouse was recorded by a video camera for 10 min. The recorded video file was later analyzed with Any-Maze software (San Diego Instruments). Time in the center of the field (a 25 x 25 cm square) was measured. The open field arena was cleaned with 70% ethanol and wiped with paper towels between each trial. 7 week old animals were P46; > 10 week old animals were P70-77. We were blind to genotype during scoring of videos.

**Elevated plus maze test.** An individual mouse was placed at the junction of the open and closed arms, facing the arm opposite to the experimenter, of an apparatus with two open arms without walls (30 x 5 x 0.5 cm) across from each other and perpendicular to two closed arms with walls (30 x 5 x 15 cm) with a center platform (5 x 5 cm), and at a height of 40 cm above the floor. The movement of the mouse was recorded by a video camera for 10 min. The recorded video file was later analyzed and time in the open arms of the apparatus was measured. The arms of the elevated plus maze apparatus was cleaned with 70% ethanol and wiped with paper towels between each trial. 7 week old animals were P45-51; > 10 week old animals were P72-121. We were blind to genotype during scoring of videos.

**Social interaction task.** Mice were connected to the EEG preamplifier, then allowed to habituate for 15 min before beginning the task. Following habituation, we recorded baseline EEG activity for 5 min. Then we introduced a juvenile mouse (3-4 weeks old) of the same gender as the subject mouse into the homecage of the subject mouse and allowed the freely moving mice to interact for 5 min while continuing to record EEG activity. We recorded EEG using a time-locked video EEG monitoring system (Pinnacle Technology), enabling us to subsequently correlate periods of social interaction (defined as sniffing, close following, and allo-grooming) with specific timepoints in the EEG recording. 7 week old animals were P46; > 10 week old animals were P70-77. We were blind to genotype during scoring of videos.

**Measuring rule-shifting performance in mice.** This task was based on the attention set-shifting task described by (Bissonette et al., 2008). Briefly, mice are single-housed and habituated to a reverse light/dark cycle and food intake is restricted until the mouse is 80-85% of the *ad libitum* feeding weight. At the start of each trial, the mouse was placed in its home cage to explore two bowls, each containing one odor and one digging medium, until it dug in one bowl, signifying a choice. The bait was a piece of a peanut butter chip (approximately 5-10 mg in weight) and the cues, either olfactory (odor) or somatosensory and visual (texture of the digging medium which hides the bait), were altered and counterbalanced. All cues were presented in small animal food bowls (All Living Things Nibble bowls, PetSmart) that were identical in color and size. Digging media were mixed with the odor (0.01% by volume) and peanut butter chip powder (0.1% by volume). All

odors were ground dried spices (McCormick garlic and coriander), and unscented digging media was purchased from Cole Hardware and Cole Valley Pets (Mosser Lee white sand, litter).

After mice reached their target weight, they underwent one day of habituation. On this day, mice were given ten consecutive trials with the baited food bowl to ascertain that they could reliably dig and that only one bowl contained food reward. All mice were able to dig for the reward. Then, on Days 1 and 2 (and in some cases, on additional days as well), mice performed the task. After the task was done for the day, the bowls were filled with different odor-medium combinations and food was evenly distributed among these bowls and given to the mouse so that the mouse would disregard any associations made earlier in the day. In our original rule-shifting experiments (shown in Fig. 3), we analyzed behavioral data from Day 2. Subsequently, when we studied how clonazepam (CLZ) affects behavior, we injected mice with vehicle on the habituation day and Day 1, and CLZ on Day 2, and analyzed behavioral data from the latter two days. We delivered vehicle and CLZ in this order because of the potentially long half-life of CLZ, its metabolites, and its effects.

Mice were tested through a series of trials. The determination of which odor and medium to pair and which side (left or right) contained the baited bowl was randomized (subject to the requirement that the same combination of pairing and side did not repeat on more than 3 consecutive trials) using <http://random.org>. On each trial, while the particular odor-medium combination present in each of the two bowls may have changed, the particular stimulus (e.g., a particular odor or medium) that signaled the presence of food reward remained constant over each portion of the task (initial association, rule

shift, and rule reversal). If the initial association paired a specific odor with food reward, then the digging medium would be considered the irrelevant dimension. The mouse is considered to have learned the initial association between stimulus and reward if it makes 8 correct choices during 10 consecutive trials. Each portion of the task ended when the mouse met this criterion. Following the initial association, the rule-shifting portion of the task began, and the particular stimulus associated with reward underwent an extra-dimensional shift. For example, if an odor had been associated with reward during the initial association, then a digging medium was associated with reward during the rule-shifting portion of the task. The mouse is considered to have learned this extra-dimensional rule shift if it makes 8 correct choices during 10 consecutive trials. Finally, during the rule reversal portion of the task, the stimulus that had been consistently not rewarded during the initial association becomes associated with reward. For example, if garlic had been associated with reward during the initial association, then during the rule reversal, coriander would become associated with reward. When a mouse makes a correct choice on a trial, it is allowed to consume the food reward before the next trial. Between trials, mice were transferred from their home cage to a holding cage while the new bowls were set up. After making an error on a trial, a mouse was transferred to the holding cage for a minimum of 60 sec. For experiments in which we delivered optogenetic stimulation to behaving mice, light stimulation began once mice reached the 80% criterion during the initial association portion of the task. Mice then performed three additional initial association trials before the rule-shifting portion of the task began. Light stimulation continued throughout the rule-shifting portion of the task. 7 week old animals were P46-52; > 10 week old animals were P80-93. We were blind to genotype during rule shifting

in 7 week old mice. We were also blind as to which mice had been injected with each virus (I12b-ChR2 vs. I12b-mCherry, DIO-Arch vs. DIO-eYFP) and to genotype (I12b-Cre-positive vs. I12bCre-negative) in the *in vivo* optogenetic experiments.

This rule shift comprises many elements of cognitive control, and while it is certainly much simpler than corresponding human tasks, it shares some of their key constructs, as elaborated by the NIMH RDoC matrix. For example, like the Switching Stroop and Wisconsin Card Sorting tasks, the rule shift requires subjects to attend to a set of stimuli that were previously irrelevant to the outcome of each trial (performance monitoring), learn a rule using those previously irrelevant stimuli (goal updating / selection), make decisions using this new rule (response selection), and suppress perseverative responses based on formerly task-relevant cues (response suppression). Deficits in these PFC-dependent cognitive domains are hallmarks of executive dysfunction in schizophrenia (Carter et al., 2012), and similar deficits occur in autism as well (Hill, 2004; Liss et al., 2001; Yerys et al., 2009). Similar tasks have been used previously in mice and depend on the mPFC (Bissonette et al., 2008; Scheggia et al., 2014). Compared to those tasks, ours has been intentionally simplified in order to make it possible to test how acute optogenetic manipulations affect cognitive flexibility, as we will describe. Thus, while our task does not necessarily lead to the formation of attentional sets as in those prior studies (Bissonette et al., 2008; Scheggia et al., 2014), it does measure key aspects of cognitive flexibility and cognitive control, as described above.

**EEG surgeries.** Surgeries were performed after mice were anesthetized with isoflurane

to an areflexive state. Conductive stainless steel screws that served as recording electrodes were implanted intracranially at the following coordinates (in millimeters relative to bregma): mPFC: +1.7 anterior-posterior (AP),  $\pm 0.6$  mediolateral (ML), -2 dorsal-ventral (DV); temporal cortex: -2.5 AP,  $\pm 3.5$  ML, -2 DV. A screw that acted as a ground electrode was also implanted at -3 AP, -3 ML, -2 DV. These screws were attached to a head mount using conductive wire, dental cement was used to secure the head mount, and animals were allowed to recover for 3-5 days before recording sessions were initiated.

**Olfactory discrimination test.** The olfactory discrimination ability of mice was examined with decreasing concentrations (100% is the amount of odorant used in the rule-shifting task) from 100%, 50%, 25% to 12.5%. On each trial, one of two bowls was baited with coriander odor and a food reward. The other bowl was baited with garlic odor and lacked food reward. Mice were tested on their ability to distinguish between decreasing concentrations of coriander versus garlic and had to achieve at least 80% success in choosing the coriander-scented (and food containing) bowl before moving onto the next decreased concentration.

**EEG recording and analysis.** Differential EEG was recorded at 1 kHz from mice that were at least 7 weeks old using a time-locked video EEG monitoring system (Pinnacle Technology). The PFC signal was the difference between left and right prefrontal electrodes. For the social interaction task, we computed power during time periods in which the subject mouse was actively engaged with the novel juvenile mouse (see

above). For the rule-shifting task, we computed power at the time when the mouse signified its choice by began to dig in a bowl  $\pm 8$  sec. We computed power in various frequency bands using time windows of 2048 (for the rodent analog of the WCST) or 4096 (for computing point at baseline or during social interaction) points and the *spectrogram* function in Matlab (Mathworks, Natick, MA). To compute the power in each band, we first multiplied the output at each frequency  $f$ , by the value of  $f$  to correct for  $1/f$  falloff, added up the power within each frequency band at each timepoint, either during the baseline period, or during the task, and compared unnormalized power (measured in log units) during the task to the power during the baseline period in wild-type and *Dlx5/6*<sup>+/-</sup> mice. In order to compare baseline power across genotypes and frequency bands in Fig. 3C, we began with the output from the *spectrogram* function, normalized by the total area under the curve (for frequencies <120 Hz, excluding 58-62 Hz) for each mouse, and averaged across all mice of one genotype.

To analyze changes in power during the baseline period (which was just before the social interaction task), we first used 2-way ANOVA and found significant effects of genotype ( $p < 0.001$ ), frequency ( $p < 0.001$ ), and genotype  $\times$  frequency ( $p < 0.05$ ). We then checked for differences between genotypes for each frequency band using two-tailed, unpaired Student's *t*-tests. For the rule-shifting task, we used repeated measures ANOVA with mouse, condition / time during task (baseline or time relative to digging), and genotype  $\times$  condition (baseline vs. task) as factors; asterisks indicate significance of the genotype  $\times$  condition interaction. For social interaction, we used repeated measures ANOVA with mouse, task condition (baseline vs. social interaction), and genotype  $\times$  condition (baseline vs. social interaction) as factors; asterisks indicate the significance of

the genotype  $\times$  condition interaction.

**Drug administration.** Clonazepam at indicated concentrations (0.0625 mg/kg  $\sim$  0.5 mg/kg, Sigma) was diluted in the vehicle solution (PBS with 0.5% methylcellulose) then injected (I.P.) in a volume of 0.01 ml/kg 30 min prior to behavioral testing.

**Dual implant surgeries.** Surgeries were performed after mice were anesthetized with isofluorane to an areflexive state. After viral injections (I12b-ChR2-eYFP, I12b-mCherry, DIO-Arch, or DIO-eYFP) in both hemispheres were completed, dual fiber-optic cannulae (Doric Lenses, Inc.) were implanted intracranially at the following coordinates (in millimeters relative to bregma): mPFC: +1.7 anterior-posterior (AP),  $\pm$ 0.35 mediolateral (ML), -2.25 dorsal-ventral (DV) for bilateral mPFC stimulation. Behavioral experiments began 5.5 weeks after the surgery, to allow time for viral expression.

**EEG and Dual implant surgeries.** Surgeries were performed after mice were anesthetized with isofluorane to an areflexive state. After viral injections (I12b-ChR2-eYFP, I12b-mCherry, DIO-Arch, or DIO-eYFP) in both hemispheres were completed, both EEG recording electrodes and dual fiber-optic cannulae (Doric Lenses, Inc.) were implanted intracranially at the following coordinates (in millimeters relative to bregma): mPFC: +1.7 anterior-posterior (AP),  $\pm$ 0.35 mediolateral (ML), -2.75 dorsal-ventral (DV) for the EEG recording electrodes and -2.25 dorsal-ventral (DV) for the fiber-optic cannulae for bilateral mPFC stimulation. A screw that acted as a ground electrode was

also implanted at -3 AP, -3 ML, -2 DV for the EEG recording setup. These screws were attached to a head mount using conductive wire, and dental cement was used to secure the head mount and dual fiber-optic cannulae. Behavioral experiments began 5.5 weeks after the surgery, to allow time for viral expression.

***In vivo* optogenetic stimulation.** ChR2 stimulation: A 473 nm blue laser (OEM Laser Systems, Inc.) was coupled to the dual fiber-optic cannulae (Doric Lenses, Inc.) through a 200 micron diameter dual fiber-optic patchcord with guiding socket (Doric Lenses, Inc.) and 1x2 intensity division fiber-optic rotary joint (Doric Lenses, Inc.), and adjusted such that the light power was ~0.5 mW total power for both fibers. A function generator (Agilent 33500B Series Waveform Generator) connected to the laser administered either 40 Hz, 5 msec pulses of light stimulation or a 125 Hz burst of 4, 4 msec pulses, repeated at 12.5 Hz during the illumination period.

Arch stimulation: A 532 nm green laser (OEM Laser Systems, Inc.) was coupled to the dual fiber-optic cannulae (Doric Lenses, Inc.) through a 200 micron diameter dual fiber-optic patchcord with guiding socket (Doric Lenses, Inc.) and 1x2 intensity division fiber-optic rotary joint (Doric Lenses, Inc.), and adjusted such that the light power was ~5.0 mW total power for both fibers. Light stimulation was constant during the illumination period.

**Statistical analysis.** Data analysis was performed in Matlab (The MathWorks) using custom written software. Student's *t* tests were used to compare pairs of groups, unless there were repeated measurements or unpaired observations, in which case ANOVA was

used. For the rule-shifting task, we computed significance for each frequency band separately using ANOVA with mouse, condition (baseline vs. task) / time during task, and condition  $\times$  genotype as factors. Error bars indicate  $\pm 1$  SEM unless otherwise specified.

To analyze changes in power in our EEG data, we computed spectrograms from completely non-overlapping time windows and compared unnormalized power (measured in log units) during the task to the power during the baseline period in wild-type and *Dlx5/6*<sup>+/-</sup> mice. During rule shifting, we analyzed EEG spectrograms obtained  $\pm 8$  sec relative to the beginning of digging.

To analyze changes in power during the baseline period (which occurred just before the social interaction task), we first used 2-way ANOVA and found significant effects of genotype ( $p < 0.001$ ), frequency ( $p < 0.001$ ), and genotype  $\times$  frequency ( $p < 0.05$ ). We then checked for differences between genotypes for each frequency band using Student's two-tailed, unpaired *t*-tests. To analyze differences in rule shifting-evoked power, we used repeated measures ANOVA with mouse, condition / time during task (baseline or time relative to digging), and genotype  $\times$  condition (baseline vs. task) as factors. We used the same approach to determine whether there were significant differences between rule-shifting evoked power in the CLZ and vehicle conditions (Figure 6D). Specifically, we analyzed data from each frequency band using repeated measures ANOVA with mouse, task condition / timepoint during the task, and drug condition (vehicle vs. CLZ)  $\times$  task condition (baseline vs. task) as factors. To analyze differences in social interaction-evoked power, we used repeated measures ANOVA with mouse, task condition (baseline vs. social interaction), and genotype  $\times$  condition (baseline

vs. social interaction) as factors; asterisks indicate the significance of the genotype × condition interaction.

## SUPPLEMENTAL REFERENCES

- Carter, C.S., Minzenberg, M., West, R., and Macdonald, A., 3rd (2012). CNTRICS imaging biomarker selections: Executive control paradigms. *Schizophr Bull* 38, 34-42.
- Depew, M.J., Liu, J.K., Long, J.E., Presley, R., Meneses, J.J., Pedersen, R.A., and Rubenstein, J.L. (1999). *Dlx5* regulates regional development of the branchial arches and sensory capsules. *Development* 126, 3831-3846.
- Hill, E.L. (2004). Executive dysfunction in autism. *Trends Cogn Sci* 8, 26-32.
- Lewandowski, M. and Martin, G.R. (1997). Cre-mediated chromosome loss in mice. *Nat Genet* 17, 223-225.
- Liss, M., Fein, D., Allen, D., Dunn, M., Feinstein, C., Morris, R., Waterhouse, L., and Rapin, I. (2001). Executive functioning in high-functioning children with autism. *J Child Psychol Psychiatry* 42, 261-270.
- Potter, G.B., Petryniak, M.A., Shevchenko, E., McKinsey, G.L., Ekker, M., and Rubenstein, J.L. (2009). Generation of Cre-transgenic mice using *Dlx1/Dlx2* enhancers and their characterization in GABAergic interneurons. *Mol Cell Neurosci* 40, 167-186.
- Rodriguez, C.I., Buchholz, F., Galloway, J., Sequerra, R., Kasper, J., Ayala, R., Stewart, A.F., and Dymecki, S.M. (2000). High-efficiency deleter mice show that *FLPe* is an alternative to Cre-loxP. *Nat Genet* 25, 139-140.
- Scheggia, D., Bebensee, A., Weinberger, D.R., and Papaleo, F. (2014). The ultimate intra-/extra-dimensional attentional set-shifting task for mice. *Biol Psychiatry* 75, 660-670.
- Yerys, B.E., Wallace, G.L., Harrison, B., Celano, M.J., Giedd, J.N., and Kenworthy, L.E. (2009). Set-shifting in children with autism spectrum disorders: reversal shifting deficits on the Intradimensional/Extradimensional Shift Test correlate with repetitive behaviors. *Autism* 13, 523-538.